Journal of Molecular Structure 1322 (2025) 140538

Contents lists available at ScienceDirect

Journal of Molecular Structure

journal homepage: www.elsevier.com/locate/molstr

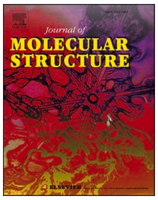

An efficient catalytic method for the Suzuki reaction and oxidation of sulfides by using novel magnetic nanoparticles ($SnFe_2O_4$) as a reusable catalyst

Ali M. Hussein [a], Jayanti Makasana [b], Suhas Ballal [c], Anjan Kumar [d,*], Bhanu Juneja [e], Piyus Kumar Pathak [f], G Sridevi [g], Salwa Bader AlReshaidan [h], Mohammed A. El-Meligy [i,l], Marwea Al-hedrewy [j,k]

[a] *Department of Biomedical Sciences, College of Applied Sciences, Cihan University-Erbil, Kurdistan Region, Iraq*
[b] *Marwadi University Research Center,Department of Chemistry, Faculty of Science Marwadi University, Rajkot 360003, Gujarat, India*
[c] *Department of Chemistry and Biochemistry, School of Sciences, JAIN (Deemed to be University), Bangalore, Karnataka, India*
[d] *Department of electronics and communication engineering, GLA University, Mathura 281406, India*
[e] *Centre for Research Impact & Outcome, Chitkara University Institute of Engineering and Technology, Chitkara University, Rajpura, 140401, Punjab, India*
[f] *Department of Applied Sciences-Chemistry, NIMS Institute of Engineering & Technology, NIMS University Rajasthan, Jaipur, India*
[g] *Department of Chemistry, Chandigarh Engineering College, Chandigarh Group of Colleges-Jhanjeri, Mohali, 140307, Punjab, India*
[h] *Department of Chemistry, Faculty of Science, King Saud University, P.O. Box 800, Riyadh 11451, Saudi Arabia*
[i] *Jadara University Research Center, Jadara University, Jordan*
[j] *College of Technical Engineering, the Islamic University, Najaf, Iraq*
[k] *College of Technical Engineering, the Islamic University of Al Diwaniyah, Al Diwaniyah, Iraq*
[l] *Applied Science Research Center, Applied Science Private University, Amman, Jordan*

ARTICLE INFO

Keywords:
Nano
Suzuki
$SnFe_2O_4$
Sulfide

ABSTRACT

In this study, we focused on the deposition of copper nanoparticles onto Cinchonine-functionalized $SnFe_2O_4$ magnetic nanoparticles. This environmentally friendly heterogeneous catalyst was thoroughly analyzed using a variety of techniques including SEM, EDS, TGA, TEM, VSM, XRD, ICP, XPS and FT-IR. In addition, it demonstrated outstanding performance as a catalyst for Suzuki reactions and the oxidation of sulfides in environmentally sustainable conditions. The catalyst could be effortlessly separated from the mixture and reused for up to four cycles without any decrease in its catalytic efficacy. This method provides the advantages of a simple procedure, high yields of products, convenient handling, environmentally friendly conditions, and short reaction times.

1. Introduction

Nanomaterials that can be magnetically separated represent a crucial class of materials with distinctive physicochemical properties, drawing the interest of numerous researchers [1–5]. Spinel ferrite compounds, as catalytic support materials, hold significant potential in industry and technology, serving as environmentally friendly catalysts in diverse organic functional group transformations and as catalytic supports [6–8]. Our recent focus on creating heterogeneous catalysts using nanomaterials led to the development of new catalytic supports functionalized with organic and inorganic ligands and complexes [9]. As we continue our research, we aim to present the spinel known as $SnFe_2O_4$ as a versatile nanomagnetic catalytic support for synthesizing a new catalyst. $SnFe_2O_4$ nanoparticles have garnered interest as heterogeneous catalysts due to their straightforward synthesis and adaptable surface properties.

Diaryls are highly valuable organic compounds widely used in the polymer, life science, and chemical industries due to their diverse applicability [10]. Many diaryls exhibit significant biological and pharmacological activities [11]. Given their importance, the development of effective synthesis methods remains a challenging and active area of research, attracting the sustained interest of researchers [12]. Among the various reported protocols, copper-based catalysts are commonly utilized for the synthesis of these compounds [13]. The most

---

* Corresponding author.
E-mail address: dashyanjan@gmail.com (A. Kumar).

https://doi.org/10.1016/j.molstruc.2024.140538
Received 24 September 2024; Received in revised form 22 October 2024; Accepted 28 October 2024

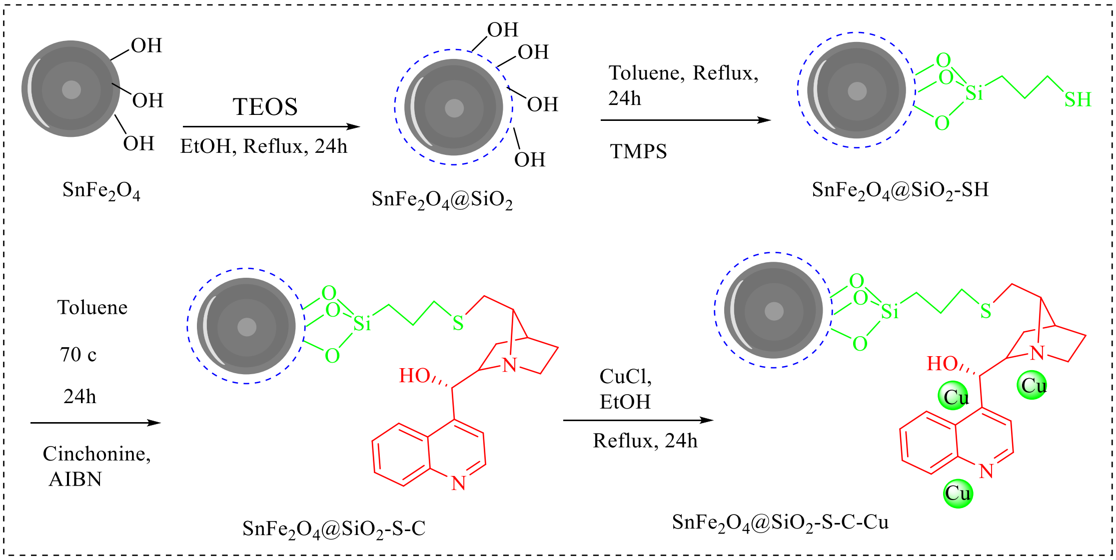

Scheme 1. Synthesis of $SnFe_2O_4@SiO_2$-S-C—Cu.

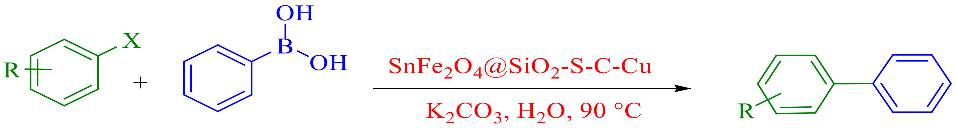

Scheme 2. $SnFe_2O_4@SiO_2$-S-C—Cu catalyzed Suzuki reactions.

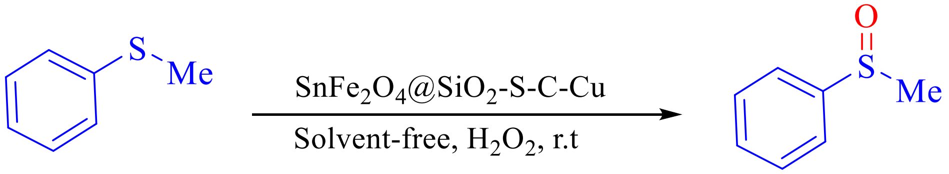

Scheme 3. Oxidation of sulfides catalyzed by $SnFe_2O_4@SiO_2$-S-C—Cu.

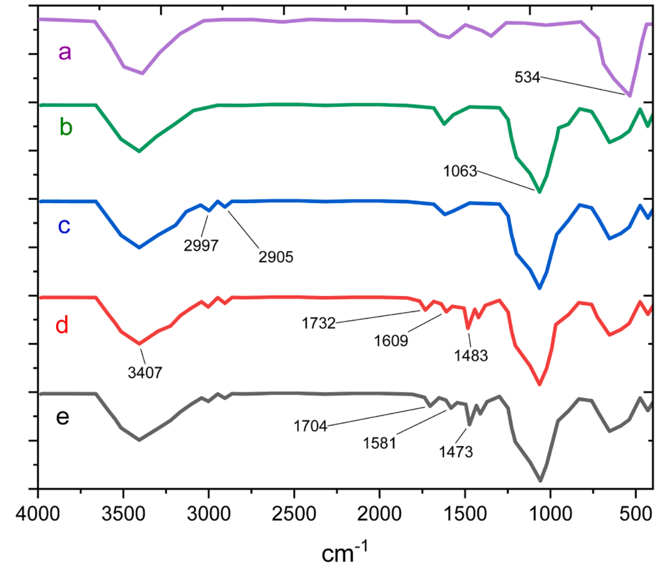

Fig. 1. Comparative study of FT-IR spectra of a) $SnFe_2O_4$, b) $SnFe_2O_4@SiO_2$, c) $SnFe_2O_4@SiO_2$-SH, d) $SnFe_2O_4@SiO_2$-S-C, e) $SnFe_2O_4@SiO_2$-S-C—Cu.

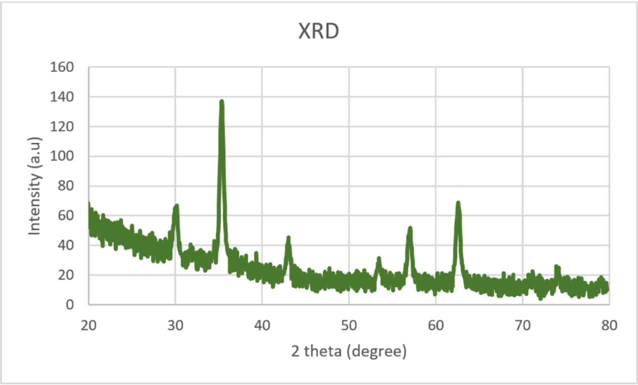

Fig. 2. XRD spectrum of $SnFe_2O_4@SiO_2$-S-C—Cu.

prevalent pathways for their generation include Pd- or Cu-catalyzed Suzuki cross-coupling. While Pd-catalyzed C—C and C—N bond formations in Ullmann reactions have shown notable progress, Cu-based catalysts are increasingly preferred due to their cost-effective raw materials, straightforward procedures, and low toxicity [10,14].

Organic sulfoxides serve as essential intermediates in a range of

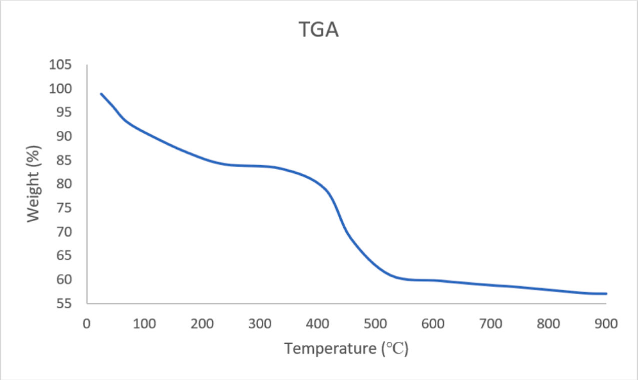

Fig. 3. TGA curve of $SnFe_2O_4@SiO_2$-S-C—Cu.

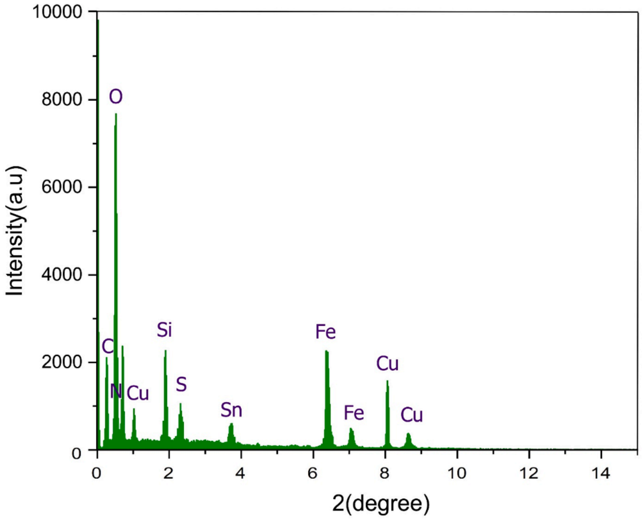

Fig. 4. EDS analysis of $SnFe_2O_4@SiO_2$-S-C—Cu.

applications across laboratories, industries, pharmaceuticals, and agrochemicals [15]. These critical compounds are generally synthesized through the oxidation of sulfides [16]. Disulfides also play a vital role in several biological and chemical processes, contributing to sensor development, oil-sweetening techniques, and functioning as vulcanizing agents [17,18].

The study presents an innovative and efficient reusable catalyst, $SnFe_2O_4@SiO_2$-S-C—Cu, which features a novel copper complex anchored on $SnFe_2O_4$. This catalyst is employed for the oxidation of sulfides and the Suzuki reaction, operating under environmentally friendly conditions.

2. Experimental

2.1. Preparation of $SnFe_2O_4@SiO_2$-S-C—Cu

The synthesis of $SnFe_2O_4@SiO_2$ began with the synthesis of $SnFe_2O_4$ following established procedures. After dispersing 1 g of $SnFe_2O_4@SiO_2$ in 30 mL of toluene through 15 min of sonication, 3 mL of (3-mercaptopropyl) trimethoxysilane was introduced to the mixture. The resulting concoction was then refluxed for 24 h. Subsequently, the obtained $SnFe_2O_4@SiO_2$-SH nanoparticles were washed four times with ethanol and isolated using magnetic decantation before being dried at 50 °C. For the next step, 1 gram of $SnFe_2O_4@SiO_2$-SH was dispersed in 30 mL of toluene through 15 min of sonication, followed by the addition of 3 mmol of cinchonine to the reaction mixture. The mixture was stirred under reflux conditions for 24 h. After that, the nanoparticles were washed multiple times with ethanol, separated through magnetic decantation, and dried at 50 °C. Following this, a thiol-ene free radical reaction occurred between the SH groups of the modified $SnFe_2O_4@SiO_2$-SH and the C = C double bond of cinchonine under the initiation of AIBN, leading to the formation of $SnFe_2O_4@SiO_2$-S-C MNPs. The Cu was finally grafted onto the heterogenized ligand by reacting 1 g of $SnFe_2O_4@SiO_2$-S-C with 3 mmol of CuCl in EtOH under reflux conditions for 24 h. Subsequently, the derived $SnFe_2O_4@SiO_2$-S-C—Cu MNPs were isolated via straightforward filtration, followed by rinsing with hot water and hot EtOH to remove any unsupported CuCl substrates, and subsequently dried at 50 °C (Scheme 1).

2.2. Preparation of C-C coupling reaction

Phenylboronic acid (1.1 mmol), aryl halides (1 mmol), potassium carbonate (1.2 mmol), and 3 ml of H_2O were combined with the $SnFe_2O_4@SiO_2$-S-C—Cu complex (0.015 g) and stirred at 90 °C in an air atmosphere. The reaction was tracked using TLC. Once completed, the mixture was cooled and filtered, then the extracts were washed with ethyl acetate and dried with 0.7 g of Na_2SO_4. After removing the solvent, the desired products were obtained with excellent yields, as shown in Scheme 2.

2.3. A general procedure for the oxidation of sulfid

In a round-bottomed flask, 1 mmol of sulfide and 0.3 mL of 33 % H_2O_2 were combined with 0.01 g of $SnFe_2O_4@SiO_2$-S-C—Cu. This mixture was stirred at 25 °C without any solvent. Once the reaction was complete, the $SnFe_2O_4@SiO_2$-S-C—Cu was removed using a magnet, and the resulting products were extracted with a mix of water and ethyl acetate. The organic phase was then dried using 1.0 g of anhydrous sodium sulfate. The solvent was evaporated to yield pure sulfoxides in excellent quantities, as depicted in Scheme 3.

2.4. Selected NMR data

4-Nitro-1,1′-biphenyl:^{1}H NMR (DMSO, 400 MHz): δ_H= 7.24 (m, 5H), 7.41 (d, J = 12 Hz, 4H) ppm.

1,1′-Biphenyl:^{1}H NMR (DMSO, 400 MHz): δ_H= 8.20 (d, J = 8 Hz, 4H), 8.03–8.09 (m, 6H) ppm.

(Methylsulfinyl)benzene:^{1}H NMR (DMSO, 400 MHz): δ_H= 7.06–7.11 (m, 5H), 2.32 (s, 3H) ppm.

(Benzylsulfinyl)benzene:^{1}H NMR (DMSO, 400 MHz): δ_H= 7.27–7.30 (m, 5H), 7.06–7.11 (m, 5H), 3.88 (s, 2H) ppm.

(Enzylsulfinyl)benzene:^{1}H NMR (DMSO, 400 MHz): δ_H= 2.19(m, 4H), 1.12 (m, 6H), ppm.

Catalyst characterizations

For the effective functionalization of $SnFe_2O_4@SiO_2$-S-C—Cu magnetic nanoparticles, FT-IR spectroscopy was employed using the KBr pellet (as illustrated in Fig. 1). The absorption bands for $SnFe_2O_4$ (Fig. 1a) and $SnFe_2O_4@SiO_2$ (Fig. 1b) matched our previous observations. In Fig. 1c, the peaks at 2905 and 2997 cm^{-1} in $SnFe_2O_4@SiO_2$-SH are linked to C–H stretching vibrations. Fig. 1d shows characteristic bands at 1483, 1609, and 1732 cm^{-1}, indicative of $SnFe_2O_4@SiO_2$-S-C. The band at 1483 cm^{-1} likely corresponds to carbon-nitrogen stretching vibrations, while the presence of bands at 3407 cm^{-1} is related to OH vibrations, ensuring successful attachment. Finally, a change in peak intensity for $SnFe_2O_4@SiO_2$-S-C—Cu indicates the nitrogen atom of the amino groups coordinating with Cu (Fig. 1e).

Fig. 2 presents the X-ray diffraction (XRD) patterns of $SnFe_2O_4@SiO_2$-S-C—Cu. The diffraction peaks are observed at positions [2 2 0], [3 1 1], [4 0 0], [4 2 2], [5 1 1], and [4 4 0], which correspond to the standard patterns of an inverse cubic spinel magnetite crystal structure. Moreover, the XRD analysis indicates that the $SnFe_2O_4$ phase is preserved despite the integration of various organic functional groups

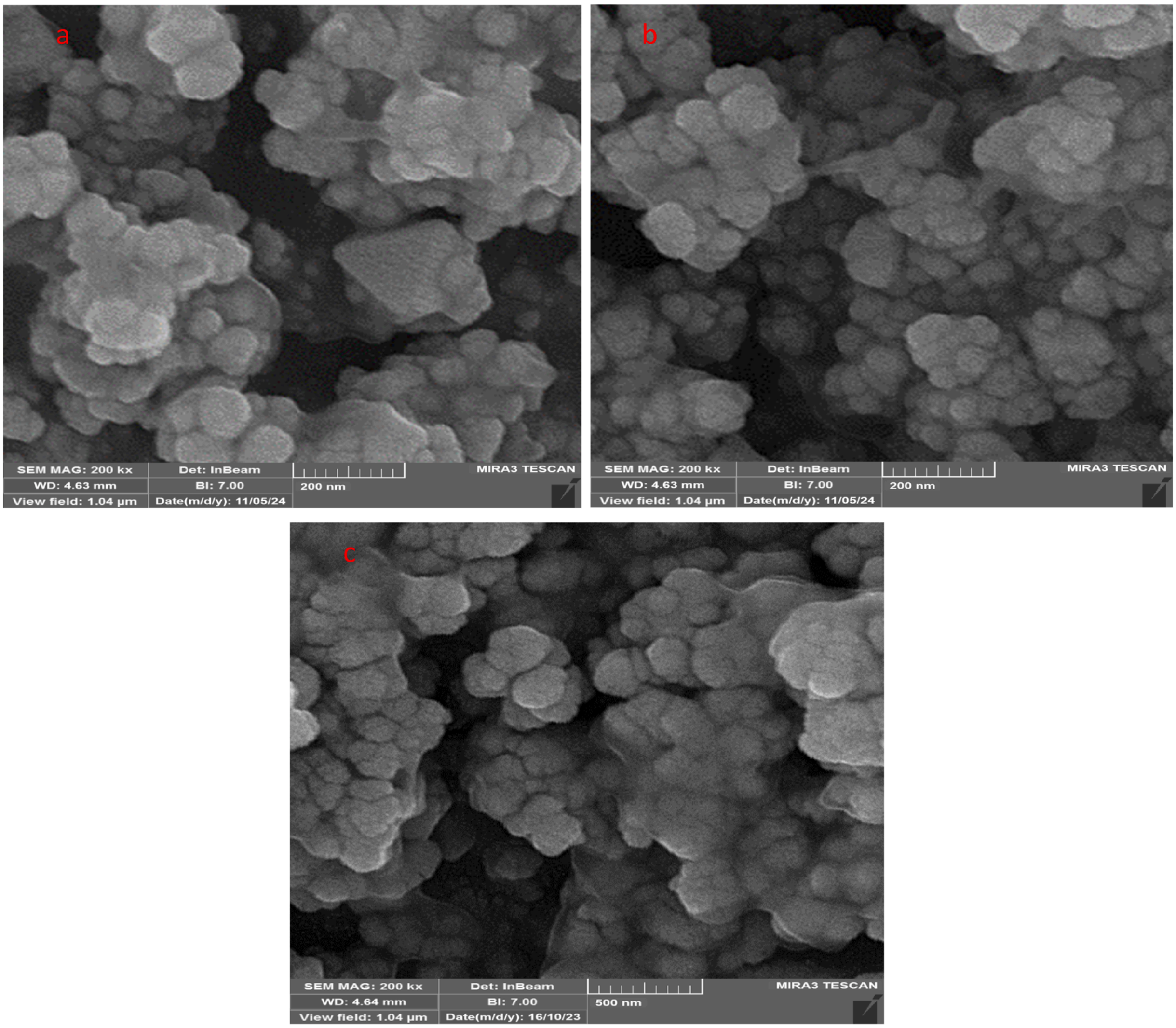

Fig. 5. SEM images of $SnFe_2O_4@SiO_2$-S-C—Cu (a and b) and recovered Catalyst (c).

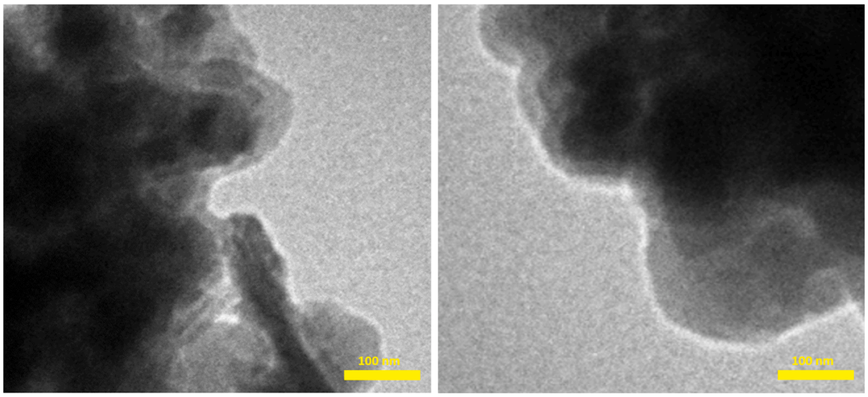

Fig. 6. TEM images of $SnFe_2O_4@SiO_2$-S-C—Cu.

during the catalyst's modification process.

The TGA analysis, illustrated in Fig. 3, was carried out to assess the thermal stability of the catalyst. In the TGA curve for $SnFe_2O_4@SiO_2$-S-C—Cu, the initial weight loss occurring below 250 °C is due to the evaporation of physically adsorbed water molecules within the compound. The subsequent weight loss between 250 and 550 °C is linked to the decomposition of the SiO_2-S-C—Cu organometallic complex situated on the surface of $SnFe_2O_4$ MNPs. Importantly, $SnFe_2O_4@SiO_2$-S-C—Cu remains stable and does not decompose, making it suitable for catalytic reactions at temperatures up to 350 °C.

The $SnFe_2O_4@SiO_2$-S-C—Cu catalyst underwent EDX analysis to identify its elemental composition. Fig. 4 verifies the presence of elements such as Sn, Si, S, N, Fe, O, Cu, and C within the catalyst, as indicated by the EDX pattern database.

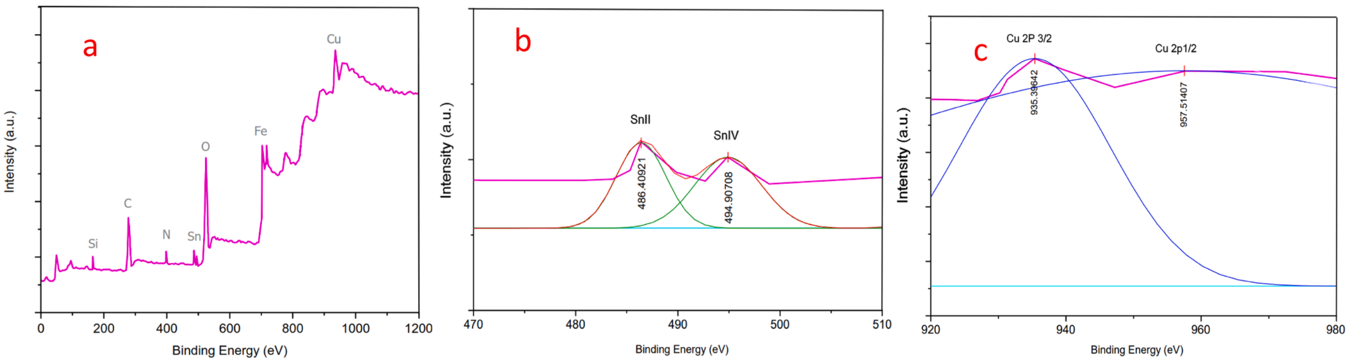

Fig. 7. XPS: $SnFe_2O_4$@SiO_2-S-C—Cu (a), Sn (b), and Cu 2p (c).

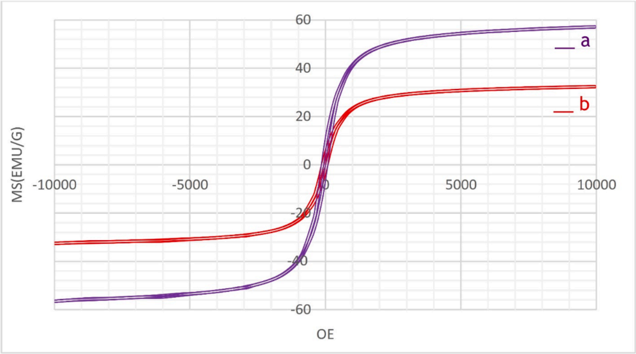

Fig. 8. VSM curves of (a) $SnFe_2O_4$ (b) $SnFe_2O_4$@SiO_2-S-C—Cu.

The SEM analysis concentrated on examining the size and morphology of $SnFe_2O_4$@SiO_2-S-C—Cu. The SEM image showed that the catalyst is composed of quasi-spherical nanoparticles, with an average diameter of about 50 ± 5 nm, as seen in Fig. 5a and b. Fig. 5c presents a comparison of the SEM spectra of the catalyst after recycling. According to the figure, the SEM analysis of $SnFe_2O_4$@SiO_2-S-C—Cu remains unchanged post-recovery, confirming the catalyst's stability under reaction conditions.

The nanoparticles' structures and morphologies were analyzed through transmission electron microscopy (TEM) (See Fig. 6). As depicted, the nanoparticles exhibited a core-shell structure, with a dark-colored core for $SnFe_2O_4$@SiO_2 nanoparticles and a light-colored shell for -S-C—Cu.

To explore the composition and chemical environment, the compound $SnFe_2O_4$@SiO_2-S-C—Cu was characterized using X-ray photoelectron spectroscopy (XPS), with findings displayed in Fig. 7. The overall survey spectra reveal the presence of Cu, Fe, O, Si, C, Sn, and N, as illustrated in Fig. 7(a). The Cu 2p region, depicted in Fig. 7(c), indicates the presence of Cu in the +1 oxidation state with binding energies of 935.3 eV for the Cu 2p3/2 energy levels. These levels are comparable to the known Cu^+ binding energy value of 957.5 eV for Cu 2p1/2. Additionally, the Sn spectra in Fig. 7(b) show binding energies of 486.4 and 494.9 eV for the Sn II and Sn IV energy levels, respectively. The XPS results confirm the successful synthesis of $SnFe_2O_4$@SiO_2-S-C—Cu.

By employing the ICP technique, we assessed the copper levels in the initial catalyst and analyzed the copper leaching after recycling. The results showed copper concentrations in both the fresh and reused nanocatalysts to be 2.0×10 $(^{-4})$ and 1.9×10 $(^{-4})$ mol. g^{-1}, respectively, indicating minimal copper leaching from the $SnFe_2O_4$@SiO_2-S-C—Cu framework.

The magnetization of both $SnFe_2O_4$ and $SnFe_2O_4$@SiO_2-S-C—Cu was examined at room temperature using a VSM, as depicted in Fig. 8. The magnetization curves demonstrated that $SnFe_2O_4$ had a saturation magnetization of 57 emu/g, while $SnFe_2O_4$@SiO_2-S-C—Cu exhibited a lower value of 25 emu/g. This reduction in saturation magnetization for the prepared catalyst is attributed to the stabilization of the S-C-Cu complex on the $SnFe_2O_4$ surface.

Catalytic studies:

3.3. Catalytic study

To fine-tune the reaction conditions, the coupling of iodobenzene with phenylboronic acid served as a model reaction. The study summarized the influence of various parameters such as base, solvent, temperature, and nanocatalyst quantity ($SnFe_2O_4$@SiO_2-S-C—Cu), with results presented in Table 1. Initially, as shown in Table 1, entry 1, the reaction was conducted without a catalyst in H_2O at 70 °C, resulting in no product formation. Subsequently, the reaction was repeated with varying amounts of $SnFe_2O_4$@SiO_2-S-C—Cu under the same conditions, which led to a substantial yield increase, reaching up to 98 % with 0.015 g of the catalyst (Table 1, entries 2–5). The next phase examined the impact of different solvents on the coupling reaction, where performing the reaction in DMF did not produce favorable results (Table 1, entries 5–9). The subsequent analysis focused on various bases used in the reaction model. Entries 10–13 in Table 1 indicated that a high yield was achieved, showing K_2CO_3 to be an effective base. Lastly, the effect of different temperatures was assessed (Table 1, entries 14, and 15), revealing that 70 °C is optimal for product formation. As shown in Table 1, the results indicate that the optimal conditions for this reaction are 0.015 g of $SnFe_2O_4$@SiO_2-S-C—Cu, 1.2 mmol of K_2CO_3 as the base, in H_2O at 70 °C.

After determining the optimal conditions for the Suzuki reaction using $SnFe_2O_4$@SiO_2-S-C—Cu as a catalyst, the activity of different aryl iodides and aryl bromides was evaluated, and the results were recorded in Table 2. All reactions showed high efficiency and generated minimal byproducts. The catalyst was particularly effective in successfully coupling aryl chlorides, aryl iodides, and aryl bromides with para, meta, and ortho groups. Additionally, the potential of $SnFe_2O_4$@SiO_2-S-C—Cu in facilitating the C—C coupling reaction between phenylboronic acid and aryl halide was examined, with the results also presented in Table 2.

A possible mechanism for the anthrax reaction has been suggested. Initially, the aryl halides undergo oxidative addition to the Cu complex, resulting in intermediate 1. Subsequently, the transmetallation of 2 leads to the formation of intermediate 3. This is then followed by reductive elimination, which restores the original $SnFe_2O_4$@SiO_2-S-C—Cu species and yields the intended product (Scheme 4).

To optimize the reaction conditions, an investigation was carried out on the oxidation process of methyl phenyl sulfide, selected as a representative compound. This study utilized H_2O_2 under various reaction parameters, including time and product yield (refer to Table 3 for detailed findings). It was noted that without $SnFe_2O_4$@SiO_2-S-C—Cu, the reaction was incomplete even after 6 h. However, by using a

Table 1
Optimizing the reaction model of iodobenzene with phenylboronic acid, using $SnFe_2O_4@SiO_2$-S-C—Cu as a catalyst.

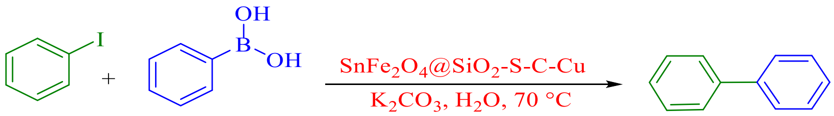

Entry	Cat. (g)	Solvent	Base	Temperature (°C)	Time (min)	Yield (%)
1	-	H_2O	K_2CO_3	70	8 h	--
2	0.008	H_2O	K_2CO_3	70	30	42
3	0.01	H_2O	K_2CO_3	70	30	84
4	0.015	H_2O	K_2CO_3	70	30	98
5	0.02	H_2O	K_2CO_3	70	30	98
6	0.015	PEG	K_2CO_3	120	30	71
7	0.015	EtOH	K_2CO_3	Reflux	30	90
8	0.015	DMF	K_2CO_3	70	30	N. R
9	0.015	DMSO	K_2CO_3	Reflux	30	95
10	0.015	H_2O	Na_2CO_3	70	30	92
11	0.015	H_2O	KOH	70	30	61
12	0.015	H_2O	CS_2CO_3	70	30	52
13	0.015	H_2O	NaOH	70	30	Trac
14	0.015	H_2O	K_2CO_3	r.t	30	N. R
15	0.015	H_2O	K_2CO_3	Reflux	30	98
16	0.015	H_2O	K_2CO_3	70	30	N. R[a]

[a] catalyst by $SnFe_2O_4@SiO_2$-S-C.

catalytic amount of $SnFe_2O_4@SiO_2$-S-C—Cu (0.01 g) in solvent-free conditions at room temperature, H_2O_2 effectively achieved full conversion of methyl phenyl sulfide to methyl phenyl sulfoxide.

This method's versatility is demonstrated by the straightforward conversion of aryl, cyclic, benzylic, and linear sulfides, as shown in Table 4. The sulfoxides were quickly obtained with high yields. To highlight the process's selectivity, sulfides with oxidation-prone and acid-sensitive functional groups such as CHO, OH, and CO_2CH_3 were used in the sulfoxidation reaction. Importantly, these functional groups remained unchanged during the conversion from sulfide to sulfoxide, as illustrated in Table 4.

Earlier research outlines Scheme 5 as introducing a possible mechanism for the oxidation of sulfides, facilitated by the catalyst $SnFe_2O_4@SiO_2$-S-C—Cu. In this catalyst, copper plays a key role as a magnetic nanocatalyst, forming the active oxidant complex. This setup aids in the transfer of oxygen to sulfur, resulting in the formation of sulfoxide.

4. Catalyst recyclability

To investigate the catalyst's durability, we analyzed the reaction between iodobenzene and phenylboronic acid as a model in ethanol, utilizing 0.015 g of $SnFe_2O_4@SiO_2$-S-C—Cu. The catalyst was easily retrieved with a magnet, as outlined in the experimental section. Moreover, $SnFe_2O_4@SiO_2$-S-C—Cu was effectively reused for four cycles without any reduction in catalytic activity, as shown in Fig. 9.

The behavior of multiple catalysts in the Suzuki reaction as reported in Table 5 of the literature reveals the superior efficiency of the $SnFe_2O_4@SiO_2$-S-C—Cu catalyst in comparison to others listed.

5. Conclusion

In this research endeavor, the synthesis of $SnFe_2O_4@SiO_2$-S-C—Cu was successfully achieved, yielding an efficient, convenient, and environmentally friendly recoverable catalyst. Characterization of the prepared catalyst was conducted through TEM, XRD, SEM, TGA, VSM, FTIR, ICP, and EDS analyses. The newly developed catalyst demonstrated its applicability in the oxidation of sulfides and Suzuki reaction. Moreover, the ease of preparation from commercially available materials further enhances the practicality of $SnFe_2O_4@SiO_2$-S-C—Cu. Notably, the catalyst exhibits advantageous traits including ease of separation, recyclability, exceptional catalytic activity, high yield, and selectivity, rendering it a proficient facilitator for both oxidation of sulfides and Suzuki reactions.

CRediT authorship contribution statement

Ali M. Hussein: Writing – original draft, Validation, Resources, Investigation. **Jayanti Makasana:** Visualization, Validation, Supervision, Software. **Suhas Ballal:** Writing – review & editing, Writing –

Table 2
Synthesis of Suzuki reaction from aryl halides using $SnFe_2O_4$@SiO_2-S-C—Cu.

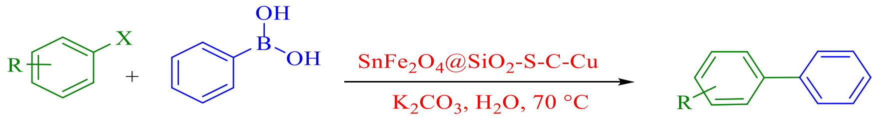

Entry	Aryl halide	Product	Time (min)	Yield (%)	TON	TOF (min^{-1})
1	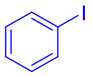	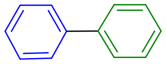	30	98	326	652
2	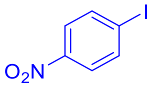	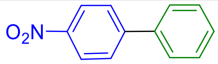	30	91	303	606
3	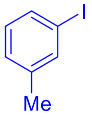	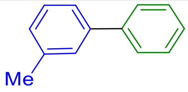	40	96	320	533
4	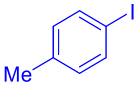	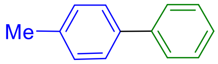	30	89	296	592
5	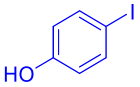	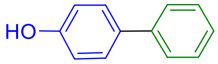	30	90	300	600
6	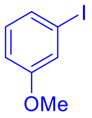	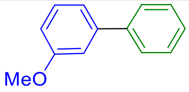	40	93	310	516
7	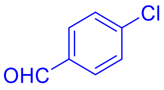	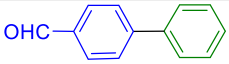	60	78	260	260
8	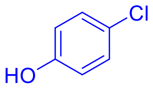	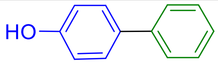	30	91	303	606
9	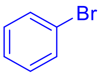	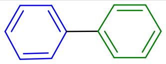	30	95	316	632
10	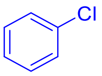	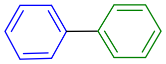	40	94	313	521
11	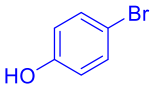	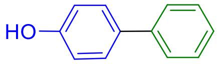	60	76	253	253
12	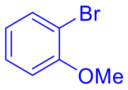	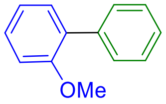	60	80	266	266

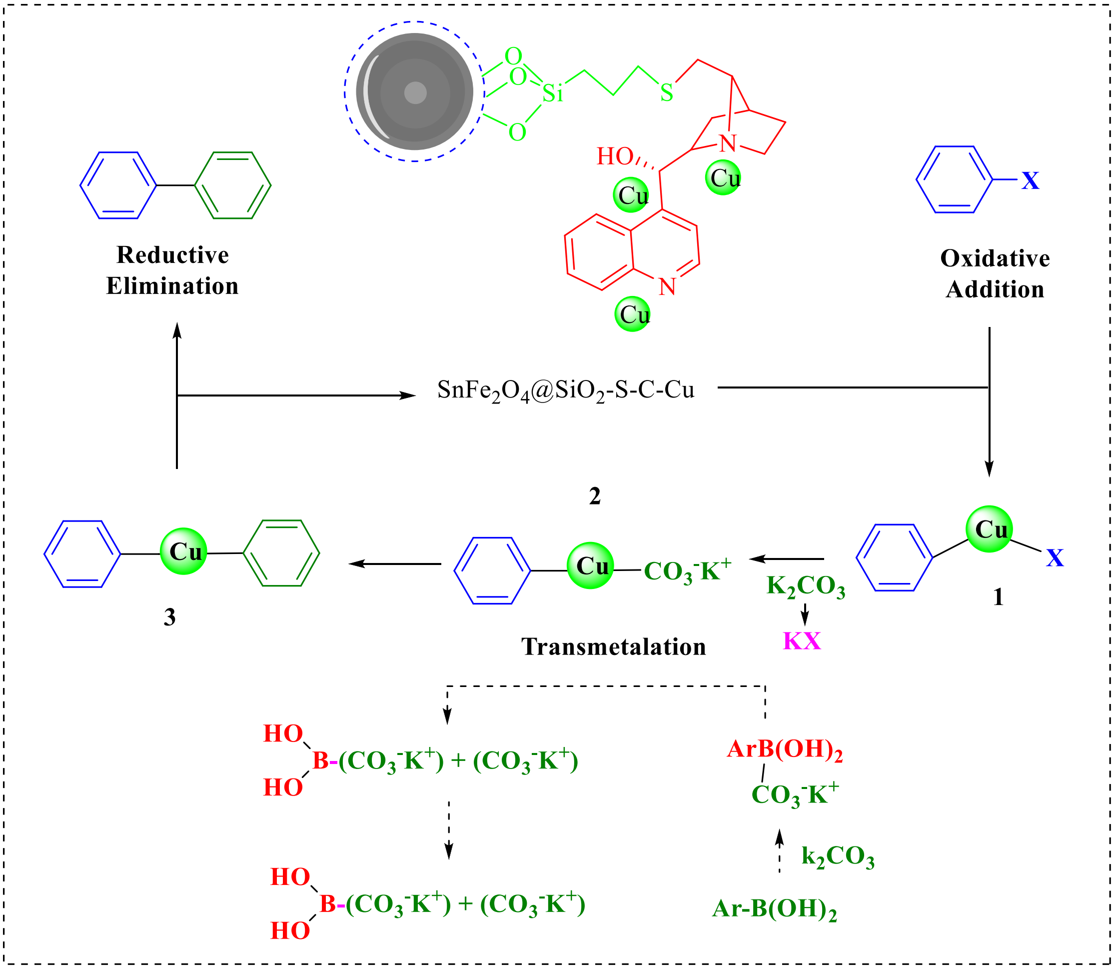

Scheme 4. Possible mechanism for Suzuki reaction.

Table 3

Optimizing the reaction conditions for the oxidation of methyl phenyl sulfide using $SnFe_2O_4@SiO_2$-S-C—Cu as a catalyst.

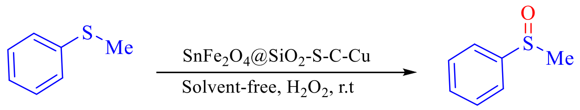

Entry	Cat. (g)	Solvent	H_2O_2 (mg)	Time (min)	Yield
1	-	Solvent-free	0.3	6h	---
2	0.005	Solvent-free	0.3	30	71
3	0.01	Solvent-free	0.3	30	98
4	0.02	Solvent-free	0.3	30	98
5	0.01	EtOH	0.3	30	45
6	0.01	PEG	0.3	30	40
7	0.01	H_2O	0.3	30	56
8	0.01	DMSO	0.3	30	80
9	0.01	Solvent-free	0.2	30	92
10	0.01	Solvent-free	0.4	30	94

Table 4

The process involves the oxidation of sulfides into sulfoxides using the catalyst $SnFe_2O_4@SiO_2$-S-C—Cu.

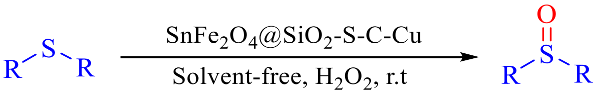

Entry	Substrate	Product	Time(min)	Yield (%)	TON	TOF (h^{-1})
1	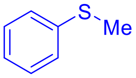	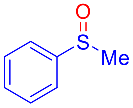	30	98	490	980
2	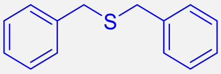	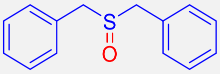	30	90	450	900
3	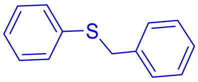	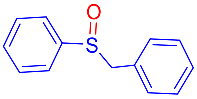	50	93	465	582
4	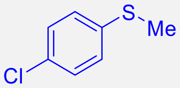	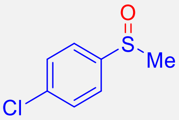	40	96	480	800
5	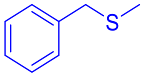	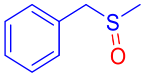	40	90	450	750
6	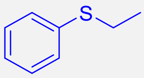	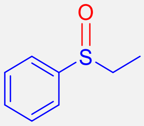	60	88	440	440
7	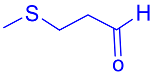	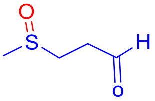	30	92	460	920
8	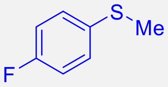	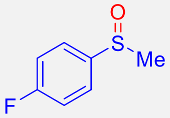	60	91	455	455
9	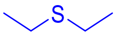	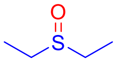	45	90	450	600
10	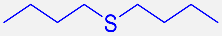	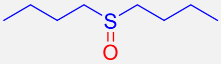	60	88	440	440

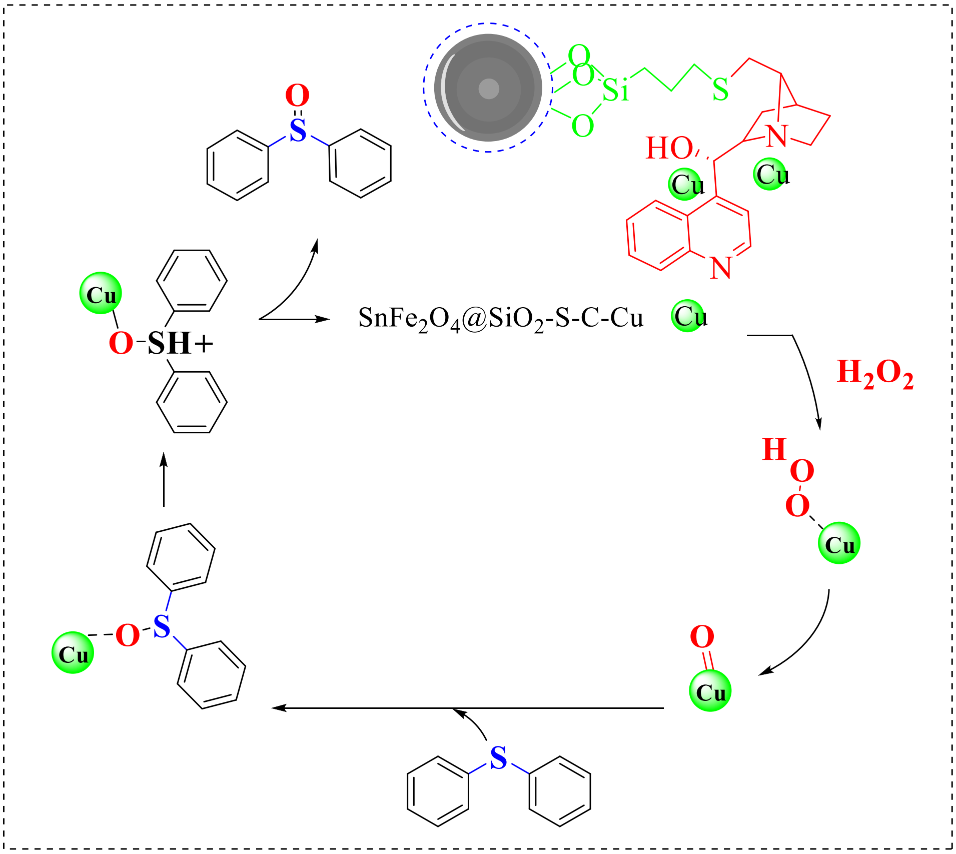

Scheme 5. The suggested mechanism for the oxidation of sulfide.

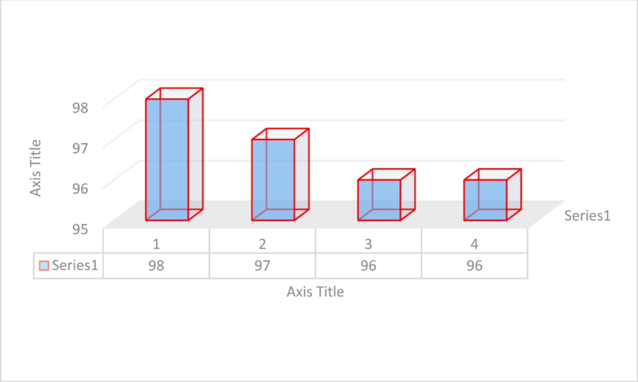

Fig. 9. The recyclability of $SnFe_2O_4@SiO_2$-S-C—Cu in the synthesis of the Suzuki reaction.

original draft, Software. **Anjan Kumar:** Validation, Software, Funding acquisition, Formal analysis, Data curation. **Bhanu Juneja:** Investigation, Formal analysis, Data curation. **Piyus Kumar Pathak:** Writing – original draft, Resources, Methodology, Investigation. **G Sridevi:** Supervision, Software, Funding acquisition, Formal analysis. **Salwa Bader AlReshaidan:** Resources, Project administration, Investigation. **Mohammed A. El-Meligy:** Writing – review & editing, Software, Data curation. **Marwea Al-hedrewy:** Supervision, Software.

Declaration of competing interest

The authors declare that they have no known competing financial interests or personal relationships that could have appeared to influence

Table 5

A comparison of the catalytic activity of $SnFe_2O_4@SiO_2$-S-C—Cu with previously reported methods in the Suzuki reaction.

Entry	Ar-X	Catalyst	Time (h)	Yield (%)	Ref
1	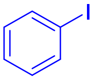	MCM-DCA-Cu	2	94	[19]
2	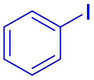	PANI-Pd	240 min	91	[20]
3	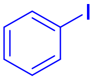	Pd/Au NPs	24	88	[21]
4	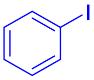	Pd NP	12	95	[22]
5	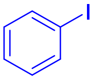	MCM-Cu	24	74	[23]
6	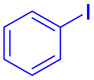	MCM-41-VO	12	100	[24]
7	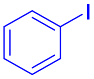	$SnFe_2O_4@SiO_2$-S-C—Cu	30	98	This work

the work reported in this paper.

Acknowledgment

The authors present their appreciation to King Saud University for funding this research through Researchers Supporting Program number (RSPD2024R779), King Saud University, Riyadh, Saudi Arabia.

Supplementary materials

Supplementary material associated with this article can be found, in the online version, at doi:10.1016/j.molstruc.2024.140538.

Data availability

No data was used for the research described in the article.

References

[1] P. Gupta, et al., Basic ionic liquid grafted on magnetic nanoparticles: an efficient and highly active recyclable catalyst for the synthesis of β-nitroalcohols and 4H-benzo[b]pyrans, J. Mol. Struct. 1274 (2023) 134351.

[2] J. Yang, et al., Microwave-assisted one-step production of biodiesel from waste cooking oil by magnetic bifunctional SrO–ZnO/MOF catalyst, J. Clean. Prod. 395 (2023) 136182.

[3] F. Qu, et al., Controlled release of Captopril by regulating the pore size and morphology of ordered mesoporous silica, Micropor. Mesopor. Mater. 92 (2006) 1–9.

[4] V. Fathi Vavsari, et al., New functionalized 8-hydroxyquinoline-5-sulfonic acid mesoporous silica (HQS-SBA-15) as an efficient catalyst for the synthesis of 2-thiohydantoin derivatives, Tetrahedron 72 (2016) 5420–5426.

[5] F. Mousavi, D. Elhamifar, S. Kargar, Copper/IL-containing magnetic nanoporous MCM-41: a powerful and highly stable nanocatalyst, Surface. Interface. 25 (2021).

[6] W. Cai, W. Zhang, Z. Chen, Magnetic Fe3O4@ZIF-8 nanoparticles as a drug release vehicle: pH-sensitive release of norfloxacin and its antibacterial activity, Colloid. Surface. B: Biointerface. 223 (2023) 113170.

[7] B. Jyothish, U.S. Geethu, J. Jacob, Influence of the Ag1+ and Co2+ doping on structural, optical and anti-cancer properties of ZnFe2O4 nanoparticles synthesized by co-precipitation method, Mater. Sci. Eng.: B 276 (2022) 115544.

[8] Y. Zong, et al., Activation of peroxymonosulfate by a magnetic Co doped NiFe2O4 catalyst for efficient Bisphenol A degradation in water, J. Taiwan Instit. Chem. Eng. 147 (2023) 104930.

[9] J.R. Sheikh, V.M. Gaikwad, V.C. Moon, S.A. Acharya, Enhancement in dielectric behavior of (Ni, Zn)Fe2O4 ferrite, in: AIP Conference Proceedings 1728, 2016.

[10] S. Jammi, et al., CuO Nanoparticles Catalyzed C−N, C−O, and C−S Cross-Coupling Reactions: scope and Mechanism, J. Org. Chem. 74 (2009) 1971–1976.

[11] D.K. Dumbre, P.R. Selvakannan, S.K. Patil, V.R. Choudhary, S.K. Bhargava, Mesoporous, ligand free Cu-Fe solid catalyst mediated CS cross coupling of thiols with aryl halides, Appl. Cataly. A: Gener. 476 (2014) 54–60.

[12] K. Buldurun, İ. Özdemir, 5-Nitrobenzimidazole containing Pd(II) catalyzed CC cross-coupling reactions: the effect of the N-substituent of the benzimidazole structure on catalyst activity, J. Mol. Struct. 1192 (2019) 172–177.

[13] Q. Gu, Q. Jia, J. Long, Z. Gao, Heterogeneous photocatalyzed C–C cross-coupling reactions under visible-light and near-infrared light irradiation, ChemCatChem 11 (2019) 669.

[14] J. Lakshmidevi, et al., Pd(5%)-KIT-6, Pd(5%)-SBA-15 and Pd(5%)-SBA-16 catalysts in water extract of pomegranate ash: a case study in heterogenization of Suzuki-Miyaura reaction under external base and ligand free conditions, Sustain. Chem. Pharm. 19 (2021) 100371.

[15] W. Ma, et al., Recent strategies for improving the catalytic activity of ultrathin transition metal sulfide nanosheets toward the oxygen evolution reaction, Mater. Today Energy 40 (2024) 101492.

[16] D. Yang, et al., A novel square-shaped Zr-substituted polyoxotungstate for the efficient catalytic oxidation of sulfide to sulfone, Chin. Chem. Lett. 109717 (2024), https://doi.org/10.1016/j.cclet.2024.109717.

[17] S.M. Islam, et al., Selective oxidation of sulfides and oxidative bromination of organic substrates catalyzed by polymer anchored Cu(II) complex, Tetrahedr. Lett. 53 (2012) 127–131.

[18] A.M. Elgorban, N. Marraiki, S.A. Ansari, A. Syed, Green synthesis of Cu/Fe3O4nanocomposite using Calendula extract and evaluation of its catalytic activity for chemoselective oxidation of sulfides to sulfoxides with aqueous hydrogen peroxide, J. Organomet. Chem. 954–955 (2021) 122077.

[19] M.M. Amini, A. Mohammadkhani, A. Bazgir, Dicarboxylic Acid-Functionalized MCM-41 with Embedded Palladium Nanoparticles as an Efficient Heterogeneous Catalyst for C–C Coupling Reactions, ChemistrySelect 3 (2018) 1439–1444.

[20] T. Scattolin, et al., Synthesis of novel allyl palladium complexes bearing purine based NHC and a water soluble phosphine and their catalytic activity in the Suzuki-Miyaura coupling in water, Appl. Organomet. Chem. 32 (2018) e4034.

[21] M. Nasrollahzadeh, A. Azarian, M. Maham, A. Ehsani, Synthesis of Au/Pd bimetallic nanoparticles and their application in the Suzuki coupling reaction, J. Ind. Eng. Chem. 21 (2015) 746–748.

[22] M. Nasrollahzadeh, S.M. Sajadi, M. Maham, Green synthesis of palladium nanoparticles using Hippophae rhamnoides Linn leaf extract and their catalytic activity for the Suzuki–Miyaura coupling in water, J. Molecul. Cataly. A: Chem. 396 (2015) 297–303.

[23] T. Das, H. Uyama, M. Nandi, Pronounced effect of pore dimension of silica support on Pd-catalyzed Suzuki coupling reaction under ambient conditions, New J. Chem. 42 (2018) 6416–6426.

[24] B. Karimi, H. Barzegar, H. Vali, Au–Pd bimetallic nanoparticles supported on a high nitrogen-rich ordered mesoporous carbon as an efficient catalyst for room temperature Ullmann coupling of aryl chlorides in aqueous media, Chem. Commun. 54 (2018) 7155–7158.